IEEE Access
Multidisciplinary ⋮ Rapid Review ⋮ Open Access Journal

Received 12 May 2022, accepted 15 June 2022, date of publication 11 July 2022, date of current version 22 July 2022.

Digital Object Identifier 10.1109/ACCESS.2022.3188992

Photonic Beamforming for 5G and Beyond: A Review of True Time Delay Devices Enabling Ultra-Wideband Beamforming for mmWave Communications

BANAFUL PAUL, (Student Member, IEEE), KUBILAY SERTEL, (Senior Member, IEEE), AND NIRU K. NAHAR, (Senior Member, IEEE)
ElectroScience Laboratory, Department of Electrical and Computer Engineering, The Ohio State University, Columbus, OH 43212, USA
Corresponding author: Banaful Paul (paul.864@osu.edu)

ABSTRACT The next generations of wireless communications are promising high capacity, low latency, and high throughput, enabled by millimeter wave spectrum. Beamforming and beam steering are key requirements for millimeter wave systems due to the fundamental limitations of such high frequencies. Traditional phased array antennas are narrow band and conventional beamforming techniques are too bulky, energy hungry, and expensive to integrate into consumer electronics. Therefore, new approaches of beamforming and beamsteering are required for 5G and beyond due to shortcomings of existing technologies. Here we present a comprehensive review of the photonic true time delay units for application in beamforming of next generations of wireless communications. The prospects and progress of several photonic techniques are discussed here along with their challenges. The fundamental focus of this endeavor will be on the on-chip Silicon-on-Insulator based approaches which enable utilizing conventional CMOS fabrication process for integration with other optical components for compact photonic integrated circuit.

INDEX TERMS Beamforming, silicon photonics, wireless communication, 5G, true time delay, mmWave, ultra wideband.

I. INTRODUCTION

The next generations of wireless communication (5G and beyond) are going to exploit the enormous spectrum of the high frequency mmWave spectrum (30 GHz-300 GHz) which promises low latency, high capacity, and throughput [1]–[4]. The current deployment of 5G mobile communication is already proving useful for solving spectrum shortages. However, it will also eventually fall short in the near future for emerging applications like autonomous driving, virtual/augmented reality (VR/AR), and the Internet of Things (IoT), requiring going beyond (6G) which plan to use spectrum above 100 GHz and extending into the higher sub-mmWave and Terahertz (THz) bands [3].

The associate editor coordinating the review of this manuscript and approving it for publication was Bilal Khawaja.

The premise of mmWave bands can only be achieved if challenges associated with higher propagation loss can be effectively addressed [1], [3], [4]. Phased array technologies enable beamforming, providing much needed gain to compensate atmospheric-losses for mmWave communications. Moreover, for mobile mmWave communications, beamforming is essential in avoiding blockages and/or utilizing non-line-of-sight channels. Real-time beamforming is thus essential for the proliferation of mobile mmWave connectivity [1], [3], [4]. Analog beam steering involves using phase shifters integrated with each antenna array. Phase shifter technology has significantly evolved in the past several decades, resulting in low-cost devices that can be packaged and integrated into array printed circuit boards (PCB) [5]–[8]. These are cheap and relatively simple to implement compared to its digital counterpart which involves challenges, such as

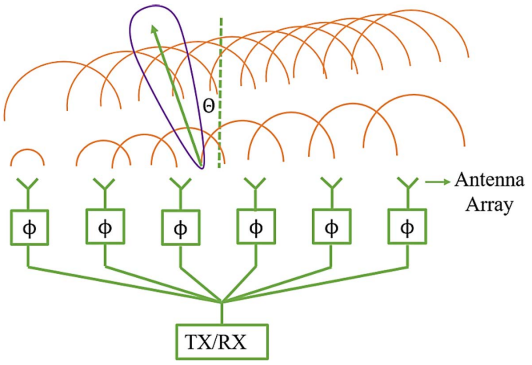

FIGURE 1. (a) Schematic demonstrating phased array antennas (PAA) transmitting (TX) or receiving (RX) signals along Θ direction due to input phase of Φ.

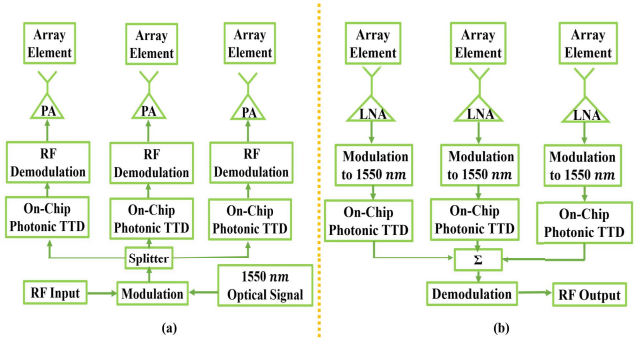

FIGURE 2. Schematic showing the (a) transmitter architecture and the (b) receiver architecture for the photonic beamforming network.

complexity, energy consumption and cost for large-scale antenna system implementation [9]. However, beam steering utilizing phase shifter technology suffers from a very well-known bottleneck, beam squinting, making it unsuitable for broadband signals [2], [10]–[12]. An effective remedy for the phase-shifter beam-squint problem is to employ true-time-delay (TTD) to introduce progressive delays independent of frequency, thereby making the beamformer inherently broadband [13], [14]. However, the high losses and bulkiness of the connecting cables of TTD units at the mmWave spectrum shadow its promises over the phase shifters using current TTD technologies [14]. This paper summarizes existing TTD technologies and proposes novel alternatives based on integrated photonic realizations if such devices harness extraordinary light-propagation modes, such as the frozen-mode. Currently, photonic TTD relaxations rely on effective integration and small form factor and this challenge can be resolved by delaying the signals in a low loss optical medium, such as photonic waveguides. The RF signal can be up-converted to the optical domain for true time delay and can be later down-converted to the RF domain before being fed to the arrayed antennas for progressive delaying. In addition to addressing the solution to a well-known bottleneck in wideband phased array systems and beam-squinting [11], photonic TTD beamforming has the added advantage of having broad bandwidth [15], [16], low loss and power consumption [17], and immunity to electromagnetic interference [18] compared to electronic counterpart.

Photonic TTD beamforming can be implemented in multitude of ways. For non-integrated photonics, several schemes have already been demonstrated based on white cell bulk optics [19]–[21], fiber Bragg gratings [22], [23], stimulated Brillouin scattering (SBS) [24], [25], stimulated Raman scattering (SRS) [26], [27], and two-dimensional array of liquid crystal [28]. On the other hand, implementations for integrated photonic TTD engines have been demonstrated utilizing waveguide Bragg gratings [29], [30], microring resonators [31]–[40], photonic crystal or periodic waveguides [41]–[47], on-chip nonlinear photonics [48], [49] and switchable waveguide delay lines [50]–[53]. The latter implementation of on-chip monolithically integrated TTD is preferred, being compact and having the opportunity to integrate with other on-chip optical components such as modulator [54], filter [55], coupler [56], [57], laser [58], and detector [59].

In this endeavor, we explore the recent progress, prospects, and advancements in the field of on-chip monolithically integrated TTD devices for applications in mm-Wave beamforming for next generations of wireless communications. The first part of the article will briefly explain the underlying physics behind the design of general TTD engines and their corresponding applications in beamforming. In the following sections, past and current advancements for each of the above-mentioned techniques of on-chip TTD devices will be presented along with their corresponding advantages compared to other techniques.

II. PHOTONIC BEAMFORMING FOR PHASED ARRAY

To enable beamforming and beamsteering in wideband phased arrays, multiple stationary antenna elements are fed individually and coherently, either via phase shifters or true time delay to synthesize a directive beam (also known as main lobe) and scan it electronically towards a desired angle [11]. As depicted in Fig. 1, a proper phase relationship of array element excitations needs to be maintained. The beamforming manifold works similarly for receive or transmit signals and enables electronic steering of the main beam by varying the input phase among the antennas. For a narrow-band phased array, beam-steering via phase control works well, however, the beam quality deteriorates quickly for wider bandwidths due to frequency dependent beam shape causing temporal pulse distortions, resulting in wider beams, and spatial/temporal distortions of resolution [60]. To address this limitation, photonic beamforming is proposed as a viable solution to realize wideband beamforming of modern phased arrays.

The architecture of the transmit/receive beamforming manifold is pictorially depicted in Fig. 2. For transmitting arrays (Fig. 2(a)), the input signal is first modulated in the optical domain at, for example, the communication wavelength of 1550 *nm*. The modulated optical signal is then controlled in

the optical waveguide where different delays are generated for each antenna element depending on the required direction of beamforming. The delayed optical signals are demodulated back into the RF domain before being fed into each antenna element of the phased array. Typically, element signals are amplified using a power amplifier (PA) right before the array antennas. For reception, as depicted in Fig. 2(b), the received signal is first amplified using a RF low noise amplifier (LNA) whose output is modulated into the optical domain for photonic TTD. The delayed signals are demodulated to retrieve the total RF signal after summing all element signals coherently. Such a photonic TTD manifold can be implemented in several ways, which is the topic of this article as detailed below.

III. PHOTONIC TTD DEVICES FOR RF AND mm Wave BEAMFORMING

Considering a light wave propagating in an optically transparent nondispersive medium of material refractive index n, the velocity (v) and the time delay (τ) are defined as,

$$v = \frac{\omega}{k} = \frac{c}{n_{eff}}$$
$$\tau = \frac{L}{v} = \frac{L}{\frac{c}{n_{eff}}} = \frac{Ln_{eff}}{c} \tag{1}$$

where L is the length of the propagation medium, c is the velocity of light, n_{eff} is the effective refractive index of the guiding medium for a given polarization and mode, k is the wave number and ω is the angular frequency.

As seen, (1) states that a long time delay can be achieved either by increasing the length (L) or by increasing by the effective refractive index (n_{eff}). In general, though simple to implement, increasing length to achieve long delay is not considered efficient as it poses challenges with continuous tunability and requires large real state for implementation such as utilizing coils of fiber-optic delay lines [61], [62]. Alternatively, a large value of refractive index indicates corresponding large delay for the propagating wave which can be achieved utilizing either material resonance or structural resonance in a dispersive media [55]. For a dispersive medium, even though phase velocity can still be expressed as (1), the pulse propagation is determined by group velocity, v_g and is expressed as the slope of the dispersion relation, viz.

$$v_g = \frac{\partial \omega}{\partial k} = c(n_{eff} + \omega \frac{dn}{d\omega})^{-1} \tag{2}$$

where $dn/d\omega$ is the dispersion of the effective refractive index of the medium. Equation (2) illustrates that in addition to the effective refractive index n_{eff}, the dispersion of $n_{eff}(\omega)$ (or group refractive index) can also be viable option for introducing a variable photonic delay. Therefore, for a strongly dispersive medium, the following condition holds [46], [47], [63],

$$\text{if } \omega \frac{dn}{d\omega} \gg n_{eff}, \text{ then } v_g \approx c(\omega \frac{dn}{d\omega})^{-1} \ll c \tag{3}$$

and the group velocity of the pulse coincides with the electromagnetic energy velocity. The most spectacular demonstration of this temporal dispersion due to material resonance in [64] resulted in a so-called "Slow Light" with $n_{eff} \sim 10^9$, yielding group velocity of 17 m/s. This sharp resonance is due to electromagnetically induced transparency (EIT) in an atomic system where the interaction of the incident light with the atomic spin excitations form dark-state polaritons. The on-chip method of achieving slow light utilizing the EIT will be discussed further later in this paper. We will focus on structural resonances and spatially periodic dispersion which are simpler to realize in compact form with better control over tunability opposed to material resonance. However, both the material and structural resonance occurs within a very narrow bandwidth. Therefore, if the Fourier transform of the short light pulse exhibits a bandwidth that is larger than the resonance bandwidth, the pulse will undergo a dispersion or phase induced distortion and this relation can be expressed as,

$$\frac{\Delta\omega}{\omega} < \frac{v_g}{c} \tag{4}$$

Finally, even though for comprehensive evaluation of the slow light, delay bandwidth product (DBP) is commonly utilized, for comparing slow wave devices with different dimensions and/or operating bandwidth, normalized delay bandwidth product (NDBP) is more appropriate whenever available [65]. DBP is defined as the product of delay time and frequency bandwidth whereas NDBP is defined and expressed as,

$$NDBP = n_g \times \frac{\Delta\omega}{\omega_0} \tag{5}$$

where, n_g is the group refractive index, ω_0 is the central frequency of light, $\Delta\omega$ is the bandwidth. Below, we describe several well-known photonic slow wave structures and discuss their properties.

A. PHOTONIC CRYSTAL WAVEGUIDES (PCW)

Originally conceptualized by Sajeev and Yablonovitch in 1987, Photonic Crystals (PC) are a class of artificial optical materials with periodic dielectric structure that gives rise to unusual optical properties including photonic bandgap, where optical frequencies are not allowed to propagate within the structure [68]–[70]. Figure 3(a) shows the scheme of a simple PC with its corresponding dispersion diagram depicted in Fig. 3(b) which is significantly different than a conventional dispersion diagram of a material, outlined in Fig. 3(c). In general, PCWs can be classified as line defect waveguide [71] or photonic crystal coupled waveguide (PCCW) [72]–[74]. By introducing defects in the PC in the form of missing array of periodic dielectrics, it is possible to guide and slow down light due to existence of bandgap along the lateral direction and a total internal reflection in the wave propagation direction [75]–[77]. However, the operating point in PCWs is usually near the band edge which takes a near-parabolic dispersion curve and causes high dispersion for optical pulses

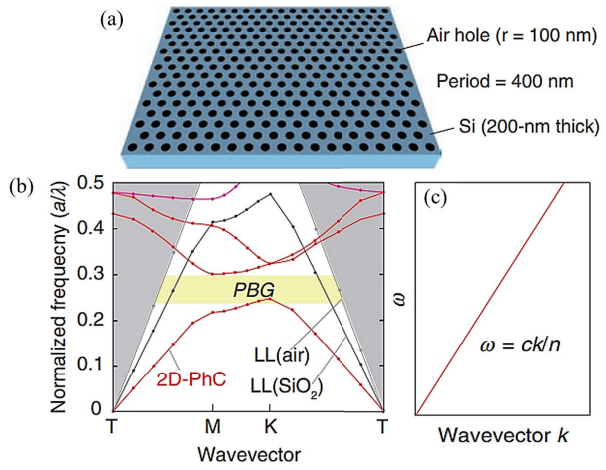

FIGURE 3. (a) Schematic of a 2D PC slab fabricated from a silicon-on-insulator (SOI) wafer. (b) Dispersion of light in the PC shown in (a). (c) Dispersion of light in conventional materials. PBG: photonic bandgap; LL: light line (adapted with permission from [66]).

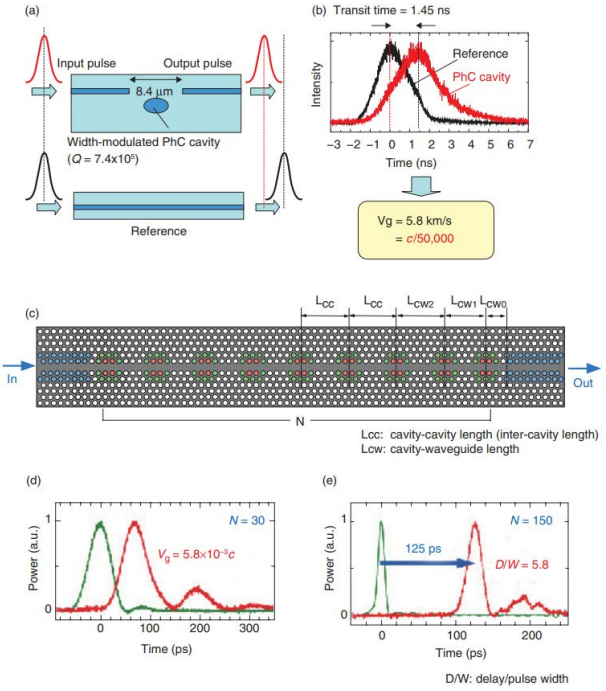

FIGURE 4. (a) Slow light in a cavity, (b) Slow light propagation in a single ultrahigh-Q nanocavity, (c) Schematic of coupled nanocavities, (d), (e) Slow light propagation in coupled nanocavities for different number of arrays. (adapted with permission from [66]).

with short duration. This regime eliminates most of the advantages of slow light due to bandwidth limitation and requires careful and crafty design engineering of PCWs with the aim of achieving wideband, low group velocity dispersion (GVD) slow light with high group refractive index, n_g [78]–[82]. This problem can be addressed by coalescing two PCWs with opposite dispersion characteristics (dispersion-compensated) slow wave devices [46], [67], [73], [83]–[86] or by utilizing zero-dispersion slow-light devices which suppress the higher order dispersion [79], [80], [82], [87]–[89].

Notomi *et al.* first demonstrated such slowing down of light in Silicon photonic crystal [90] and spurred demonstration of PC waveguides [91], [92]. Nishikawa *et al.* demonstrated an early TTD device in 2002 by utilizing an impurity band in defect coupled PCW on SOI platform and achieved 600 fs delay within a length of 20 μm at 1.55 μm [93], [94]. Vlasov *et al.* demonstrated 300 fold reduction of group velocity on SOI platform along with active tuning of the refractive index of the device employing integrated heater [43]. Notomi *et al.* demonstrated a delay line depicted in Fig. 4(a) and (b) by utilizing ultrahigh-Q nanocavity in photonic crystals with an optical delay of 1.53 ns corresponding to c/50,000 [95].

Even though this is the highest delay achieved on all-dielectric system so far, from practical application perspectives, devices with wider bandwidth will be much more useful as opposed to such ultrahigh-Q resonator devices. To this end, Mori and Baba proposed a chirped PCW to form a unique flat band of coupled modes in the photonic band gap [83], [84]. The device was later realized and verified for the first time by Huang and Notomi with measured group delay corresponding to c/60 [73]. Notomi *et al.* later extended this for a large scale (N>100) array of ultrahigh-Q coupled nanocavities as depicted in Fig. 4(c). For a 1 nm bandwidth of input optical pulse, this particular device achieved lowest group velocity corresponding to c/170 and highest delay of 125 ps, depicted respectively in Fig. 4(d) and (e) [96].

In 2008, Mori and Baba reported a PCCW with a record high delay-bandwidth product (DBP) product of 57 (bandwidth of 1.4 THz and a 40 ps delay) with observation of $\sim$ 1 ps optical pulse transmission on the SOI substrate [67]. Figure 5(a) and (b) depict the device, whereas Fig. 5(c) outlines the flatband. They successfully demonstrated that utilizing laser heating to change the refractive index as an external controlling, the slow light pulse can be delayed by 23 ps.

Baba and Notomi later presented an improved version of this device in 2011 by utilizing higher electron-beam extraction voltage with 72 ps tunable delay for 2 ps wide pulse (fractional delay 36) which was further enhanced to 110 by compressing the output pulses through self-phase modulation and dispersion compensation in external fibers [97]. Later in 2012, they integrated multi-heaters to optimize heating power and adjust the index distribution to compensate for fabrication errors. The device enabled continuous tunable range from -32 to 54 ps/*nm*/mm with quadratic chirp generating arbitrary group delay dispersion within a 3 *nm* bandwidth around 1550 *nm* [98]. Sancho *et al.* also demonstrated a PC delay line in 2012 with tunability of 70 ps and spectral band 0-50 GHz for integrated microwave filter [41].

Recently, our group proposed a novel technique for ultra wideband delay line utilizing a much simpler and robust form of PC, allowing coupling among periodic ridge

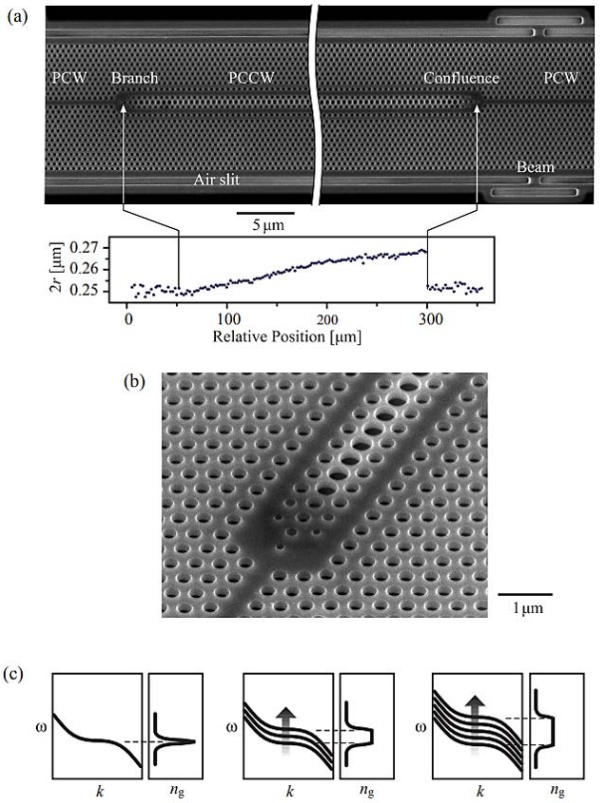

FIGURE 5. (a) Scanning electron microscope image of the PCCW device with I/O PCWs fabricated on a SOI substrate with airhole diameter 2r. (b) Magnified image of the branch between the input PCW and PCCW. (c) Group index and dispersion diagram of unchirped structure (left) and chirped structures (center and right) showing band-shift of frequencies with airhole diameter (adapted with permission from [67]).

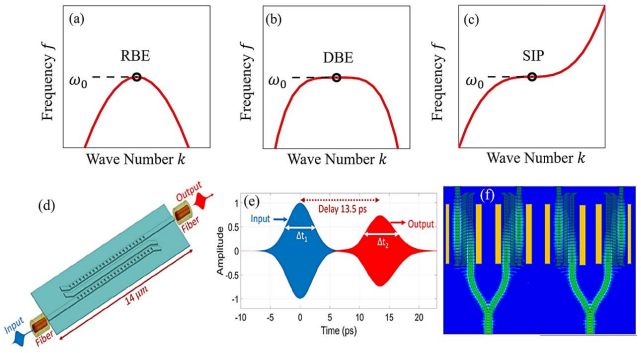

FIGURE 6. Dispersion relations portraying different stationary points: (a) a regular band edge (RBE), (b) a degenerate band edge (DBE), (c) a stationary inflection point (SIP), (d) Device schematic for coupled Si ridge waveguides to achieve SIP (e) Corresponding group delay for a propagating pulse (f) Scheme for integrated and tunable TTD employing thermal modulation for 4 channels of unit TTD, where the golden bars present the electrodes, placed on both sides of the 4 channels for thermal modulation of the spiralling slow light (adapted with permission from [99], [100]).

waveguides [45], [99], [101]. Extraordinarily-slow or frozen-modes stemming from mode degeneracy in anisotropic magnetic photonic composites have been demonstrated before which are only enabled by the simultaneous breakdown of time and space inversion symmetries requiring biased magnetic materials [102], [103]. Previously, Figotin and Vitebskiy extensively discussed the theoritical aspect of slow waves based on magnetic photonic crystals [63], [100], whereas Sertel *et al.* demonstrated several applications of this unique phenomenon in RF domain [102]–[108]. Regular band edge (RBE), depicted in Figure 6(a), is the simplest exceptional point of degeneracy (EPD) that exists at the band edge of a periodic structure when two eigenmodes coalesce to give rise to a second-order eigenwave degeneracy, $(\omega-\omega_0) \propto (k-k_0)^2$, where ω and k are wave number and frequency with ω_0 and k_0 being corresponding band edge parameters. Similarly, the degenerate band edge (DBE) requires coalescing of four Floquet-Bloch eigenwaves with dispersion relation, $(\omega-\omega_0) \propto (k-k_0)^4$ and is depicted in Fig. 6(b). Reano *et al.* analyzed and demonstrated coupled periodic optical waveguides exhibiting slow light resonance associated with DBE which could be utilized as slow wave devices [109], [110]. Finally, the stationary inflection point (SIP) or frozen mode is depicted in Fig. 6(c) which is a third-order degeneracy with dispersion relation, $(\omega-\omega_0) \propto (k-k_0)^3$. It is showed that the same frozen-mode phenomena of biased magnetic materials can be more readily achieved in all-dielectric 3-way coupled waveguides to exhibit a maximally-flat behavior within the propagation band, giving rise to SIP. The device schematic is depicted in Fig. 6(d) and Fig. 6(e) demonstrates that it enables a 5 ps pulse at 1.55 μm (193.4 THz) to have a delay-bandwidth product of 6.75 along with unprecedented frequency independent bandwidth of about 0.5 THz for RF-mmWave–THz beamforming. It translates into slowing down light wave over c/600 compared to free space. Figure 6(f) depicts the device schematic for a TTD beamforming network with thermal tunability of each channel for on-chip integration.

B. COUPLED MICRORING RESONATOR (MRR) WAVEGUIDE

Weakly coupled resonators in a periodic chain can support a Bloch excitation with significantly lowered group velocity which is true irrespective of the nature of individual resonators [63], [100]. The group velocity in a resonant cavity decreases proportionately to the cavity finesse (i.e. Quality factor, or Q-factor), which is defined as the ratio of the fundamental mode spacing (or free spectral range (FSR)) and full-width half maximum (FWHM) bandwidth of the resonances. This reduction in velocity increases the intensity of the propagating field to conserve the energy flux but reduces the bandwidth, thereby requiring cascading of resonators to have large delays utilizing a ripple-free wide passband [112], [113]. This forms the basis for slowing down of light utilizing coupled MRR waveguides for TTD in the optical domain. The earlier demonstrations of MRR structures utilized either direct coupling among MRRs (also known as Coupled Ring Resonator Waveguides (CROW), originally proposed by Yariv. *et al.* [114]) or by using a common bus (also known as side coupled integrated spaced sequence

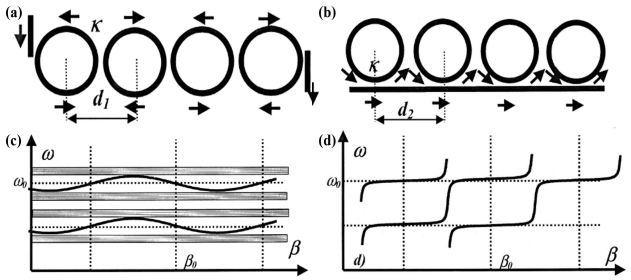

FIGURE 7. Two different slow-wave structures (a) CROW and (b) SCISSOR and their corresponding dispersion diagrams (c) and (d). (adapted with permission from [111]).

of resonator (SCISSOR)) as depicted in Fig. 7(a) and (b) respectively [47], [111], [112], [115]–[117]. The dispersion diagrams in Fig. 7(c) and (d) illustrate one fundamental difference between these two structures: the presence of band gap for CROW in Fig. 7(c) due to the existence of forward and backward propagating waves, whereas SCISSOR supports only forward propagating waves and thereby eliminates the band gap. In addition, localization and significant performance degradation in terms of achievable delay is observed in CROW structures as opposed to SCISSOR due to inevitable dissemination of the resonator parameters of fabricated CROW structures [118]–[120].

In CROW, light is slowed down due to forced recirculation of light through the coupled MRRs [114], the propagation of which has been described employing either transfer matrix method [122] or tight binding approximation [123]. Even though earlier demonstrations of CROW have been shown on Silicon-Oxynitride (SiON) [124]–[126], polymers (PMMA) [127] and Hydex glass [128] platforms, demonstrations on Silicon-on-Insulator (SOI) platform [121], [129]–[133] enabled several remarkable technological breakthrough. Due to high refractive index contrast between core and cladding ($\Delta n = 140\%$), SOI platform enabled unprecedented level of integration ($4\ \mu m^2/ring$), high FSR (up to 10 THz) [117], higher thermal efficiency for tunable delay lines due to better thermo-optic properties of silicon (dn/dT is $1.8 \times 10^{-4} K^{-1}$ at 300 K for 1550 nm) [134], lower power consumption (<50 μW/GHz), faster time response (about 10 μs) and very low thermal cross talk compared to glass-based platforms [135], [136]. In addition, SOI platform enables realization of PIN junction for excellent fast resonance frequency tuning due to carrier depletion and injection, making the response time about 20 ps [117].

During 2001 to 2007, several researchers including but not limited to Morichetti, Melloni, Poon, Mookherjea and Yariv performed in-depth theoretical investigation of CROW slow-wave structures [112], [119], [120], [122], [123]. Concurrently, Morichetti *et al.* devised a continuously tunable CROW with discrete rings, combining a digital gating scheme as depicted in Figure 8(a) along with its group delay characteristics in 8(b) [137], [138]. In 2007, Xia *et al.* demonstrated delay line with 100 MRRs achieving 500 ps delay with large fractional group delay exceeding 10 bits for bit rates as high

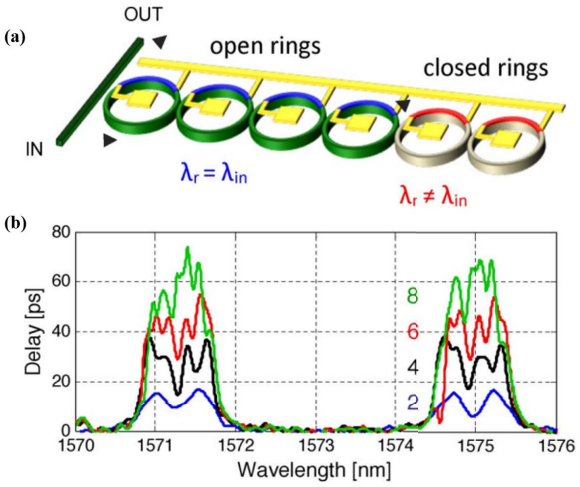

FIGURE 8. (a) Sketch of the reflective tunable CROW delay line where individual heaters on the rings can be addressed individually. (b) Group delay characteristic of the CROW along with the number of open rings (adapted with permission from [121]).

as 20 Gbps [130]. Later in 2010, Cooper *et al.* demonstrated CROW with the highest 235 MRRs without localization over frequency bands spanning several hundred gigahertz [139]. Although the implementation of doped rib waveguide for PIN junction to enable faster resonance frequency control is realizable in CROW (response time around 20 ps) [117], the adoption of rib waveguide weakens the mode confinement which increases the bending radii. Therefore, many of the state of the art demonstrations are focused more on SCISSOR scheme.

In SCISSOR, the separation between the waveguide and the resonators is kept close enough to enable evanescent coupling but negligible direct coupling among the resonators is ensured. Heebner and Boyd performed the initial analysis of SCISSOR [47], [116], [142] and showed that the total delay in the system is the sum of delay in each individual ring coupled to the common waveguide. This results in a delay-bandwidth product proportional to the number of rings and increased delay without any change in the bandwidth [47]. In 2009, Khurgin and Morton proposed and analyzed balanced SCISSOR in which resonance pairs are tuned centering the signal frequency of interest to mitigate the detrimental effect of group delay dispersion in conventional SCISSOR along with enabling wide bandwidth and continuous tunability [143]. In 2010, Cardenas *et al.* demonstrated SCISSOR with eight racetrack resonators that enabled thermally tunable optical delay with 10 GHz bandwidth and peak delay of 135 ps [31]. Ring resonators with slightly up or down shifted resonant frequencies are placed on the opposite side of the common bus waveguide as depicted Fig. 9(a) with resulting spectrum shown in Fig. 9(b). Later in 2012, Morton *et al.* further improved the device performance with increased delay of 345 ps with low distortion for a 45 ps (10.5 GHz) optical pulse and fast thermal switching of 10 μs [144]. Xie *et al.* in 2014 demonstrated a reflective-type SCISSOR by attaching a Sagnac loop at the end which can

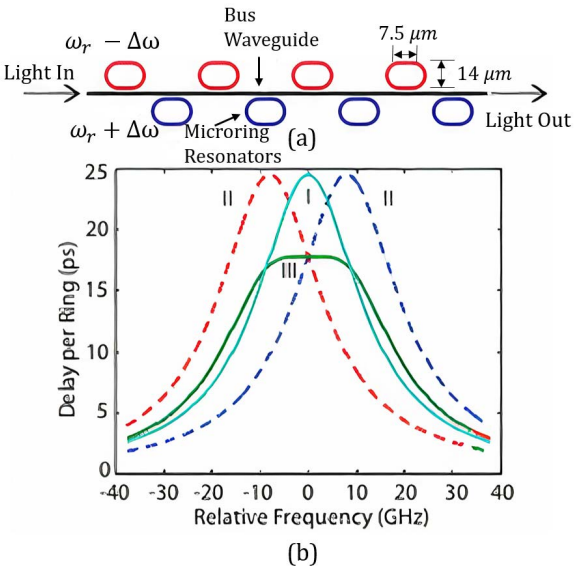

FIGURE 9. (a) Tunable delay line structure with overall central frequency ω_r (b) Simulated delay spectra of balanced SCISSOR structure from (a): (I) delay spectra with all rings aligned to ω_r; (II) delay spectra of red and blue shifted rings; (III) delay spectra for complete device. (adapted with permission from [31]).

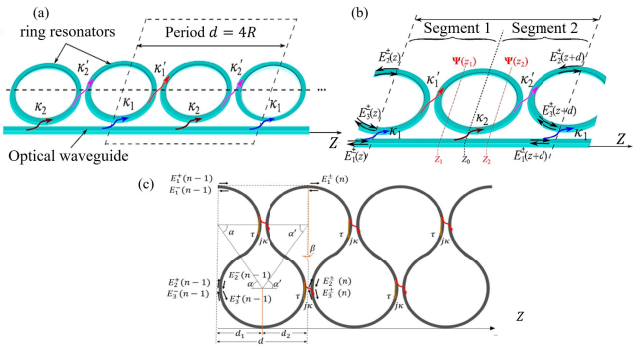

FIGURE 10. (a) Chain of coupled ring resonators of radius R side-coupled to straight optical waveguide. The field coupling coefficients between the straight waveguide and the rings alternate between k_1 and k_2, whereas between the coupled ring resonators alternate between k_1' and k_2', (b) The unit cell of this CROW with the electric field wave amplitudes defined at the cell boundaries (adapted with permission from [140]), (c) Periodic ASOW. (adapted with permission from [141]).

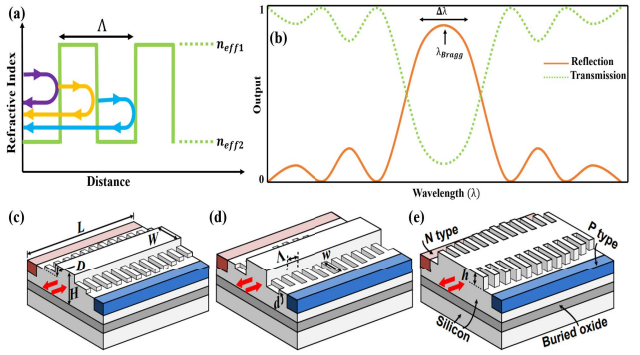

FIGURE 11. (a), (b) Reflection of signals from each interface of periodically modulated refractive index n_{eff1} and n_{eff2} (c) mesa-type (d) grooved-type and (e) chirped raised-cosine-type tunable optical delay lines on SOI. (adapted with permission from [147]).

potentially buffer 18 bits with 100 ps continuous tunability utilizing a p-i-p type micro-heater with a power tuning efficiency of 0.34 ps/mW [145]. Even though longer delays can be achieved by increasing the number of rings, this also increases the corresponding loss. To address losses, Xiang *et al.* in 2018 demonstrated low-loss continuously tunable optical delay lines based on Si_3N_4 ring resonators. This approach achieved a large delay tuning range of 3.4 ns utilizing the balanced SCISSOR for bandwidth over 10 GHz and record loss of only. 89 dB/ns [38].

Recently, Yada and Capolino proposed that a slight variation and proper parameter tuning of the CROW structure can result in a unique slow wave device by utilizing an EPD at which two or more system eigenmodes coalesce in both eigenvalues and eigenvectors [140], [141], [146]. The proposed CROW is shown in Figure 10(a) and (b). Introducing symmetry breaking in a conventional CROW through periodic coupling to an adjacent uniform optical waveguide gives rise to these EPDs leading to unique modal characteristics otherwise unavailable in regular CROW [140]. More recently, a periodic asymmetric serpentine optical waveguide (ASOW) with broken longitudinal symmetry was also proposed as shown in Fig. 10(c) due to different coupling among forward and backward propagating waves within the unit cell [141]. At the EPDs, group velocity is $\delta\omega/\delta k = 0$, with significantly reduced group velocity in the vicinity which could be utilized for efficient true time delay engines.

C. WAVEGUIDE BRAGG GRATING

A Bragg grating (BG) is an optical device with periodic variation of the effective refractive index (by varying either material or physical dimensions of the waveguide), which enables it to reflect a particular wavelength of light while allowing other wavelengths to pass [148]. Depicted in Figure 11(a) and (b), reflected signals from each interface of the high (n_{eff1}) and low refractive index (n_{eff2}) of the grating, interfere constructively within a narrow band ($\Delta\lambda$) around one particular wavelength known as Bragg wavelength and is given by, $\lambda_{Bragg} = 2\Lambda n_{eff}$, where Λ is the grating period and n_{eff} is the effective refractive index of the system.

In 1978, Hill *et al.* discovered the fiber Bragg gratings (FBGs) and revolutionized the fields of optical fiber sensing, microwave photonics and telecommunications [149]. In 2001, Murphy *et al.* extended this and demonstrated the on chip integrated-optical Bragg grating filter on the SOI platform with a bandwidth of 15 GHz (0.12 nm) for a 4 mm long grating [150]. As can be seen from the bandwidth of 0.12 nm, uniform gratings are not practical for application as true time delay devices, which typically requires much wider bandwidths. Rather, chirped BG are employed for delay line where the grating period is chirped along the way

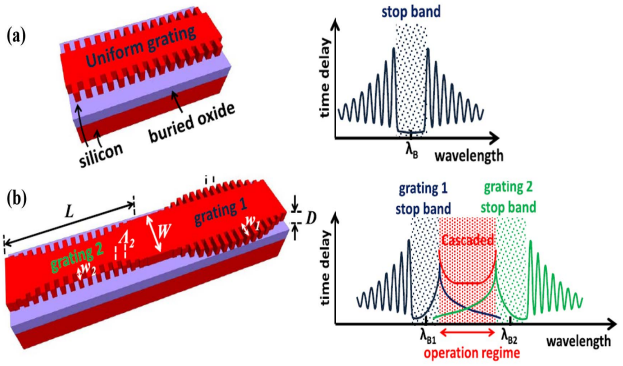

FIGURE 12. (a) Schematic of a standard grating waveguide and its delay spectrum. (b) Schematic of cascaded complementary apodized gratings, using an outward-apodized grating (grating 1) and an inward-apodized grating (grating 2). The delay spectra of gratings 1 and 2 are shown in blue and green, respectively. The combined delay spectrum of the cascaded device is shown in red (adapted with permission from [152]).

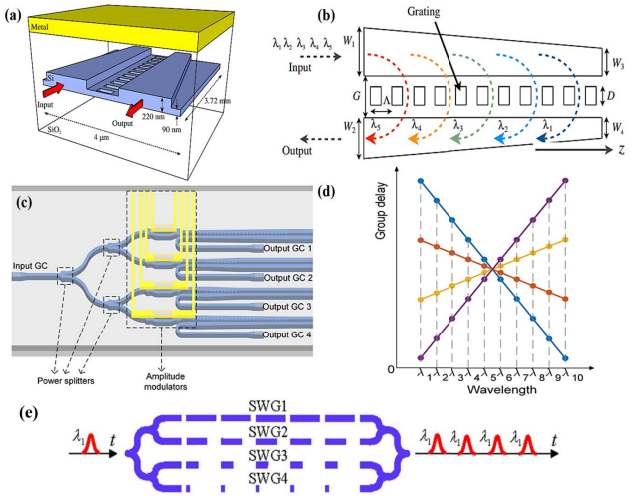

FIGURE 13. Schematic of the tunable nanophotonic delay line using contradirectional couplers with uniform Bragg gratings: (a) perspective view and (b) top view (adapted with permission from [153]) (c) Scheme of the true time delay network utilizing both positive and negative dispersion coefficients (d) The expected delay curves of the time delay network (adapted with permission from [154]) (e) Schematic of TTD based on SWG (adapted with permission from [161]).

of propagation of light which enable different wavelengths to be reflected at different positions along the grating length and thus realize different consequent delays among them. In 2011, Khan *et al.* proposed an electronically tunable optical true time delay utilizing a combination of free-carrier plasma effect and apodised gratings [147]. Figure 11(c), (d) and (e) depict three variations of the scheme employing mesa-type, grooved-type and chirped raised-cosine-type apodization respectively along with p- and n- doped regions to change the refractive index under forward or reverse bias. The device achieved tuning as high as $\sim$ 660 ps along with a loss $<$ 2.2 dB. The grooved-type devices operated at $>$ 20 Gb/s with a tunable delay of $\sim$ 40 ps. Giuntoni *et al.* realized another variation of continuously tunable delay line by employing tapered BG and thermo-optic effect which achieved a tuning range of 450 ps along with tuning coefficient of -51 ps/°C [30].

In 2013, Khan *et al.* demonstrated for the first time two cascaded apodized grating waveguides with inward and outward super-Gaussian apodization profile that achieved true time delays of 82 ps along with a tuning range of 32 ps which could potentially operate at highest bit rate of 107 Gb/s. [151].

Figure 12(a) depicts a uniform BG with its corresponding delay spectrum which reflects ripples above and below the stop band. Cascading of complementary inward and outward apodized super-Gaussian grating creates an operation regime with relatively flattened dispersion relation, portrayed in Fig. 12(b). Concurrently, they also reported that using only inward apodized super-Gaussian gratings, the TTD can have time delays as long as 132 ps with tuning range of $\sim$ 86 ps, albeit at the expense of lower bit rate of $\sim$ 13 Gb/s [152]. It is even possible to have delays as high as 220 ps with tuning range of 174 ps with lower bit rates. In 2014, Shi *et al.* realized a tunable nanophotonic delay line utilizing linearly chirped uniform Bragg gratings with contradirectional couplers which enables add-drop operation circumventing the need for optical circulators [153]. Fig. 13(a) depicts the slab perturbed rib waveguide gratings whereas Fig. 13(b) depicts the realization of index chirping through linear tapering of the rib widths. This enables input signals of different wavelengths to couple backward to the output waveguide at different distances, thus creating distinct delays. Continuous tuning of group delay up to 96 ps has been achieved along with $<$ 2 dB of insertion loss. In addition, negative chromatic dispersion of -11 ps/nm allowed for bit rates up to 100 Gb/s at the maximal delay. Recently, Zhang *et al.* extended this with both positive and negative dispersion with grating-assisted contradirectional coupler, assisted by index chirp engineering and asymmetric apodization, depicted in Fig. 13(c) and (d) [154]. Employing a 4 channel time delay network, the measured dispersion coefficient of each channel is 10.35, 4.00, -4.32 and -14.38 ps/nm with 7 nm available bandwidth which could enable beam scanning angle ranging from 36.4° to -33.9° for the beam steering.

Recently, Chen *et al.* demonstrated true time delay devices based on sub-wavelength grating (SWG) which is similar to BG except with a period (denoted Λ) that is small enough to suppress the diffraction effects and behaves as a homogeneous medium with an equivalent refractive index. It has found several applications for on-chip light manipulation, i.e., waveguide crossings [155], bends [156], couplers [156]–[158] and ring resonators [159]. As depicted in Fig. 13(e), by varying the grating period, different effective refractive index can be achieved in each line and thus distinct delays can be achieved. In 2020, they demonstrated a discretely tunable TTD using a serial array of 10 SWG waveguide BGs with a total time delay $\sim$60 ps in steps of $\sim$6.6 ps over an operating bandwidth of 41.7 nm [154]. Later in 2021, they extended it to 40 SWG waveguides in SOI

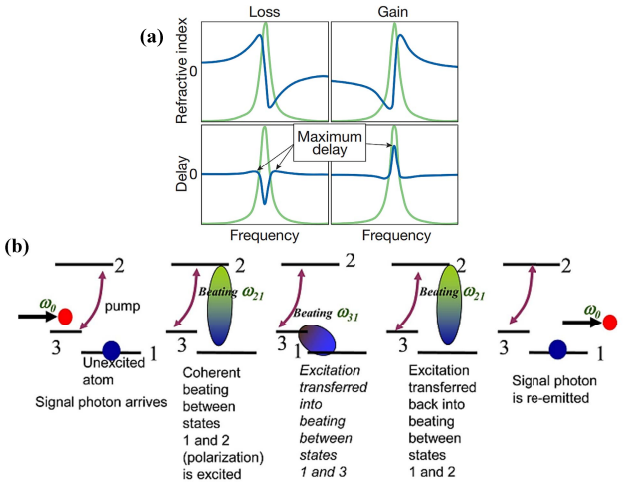

FIGURE 14. (a) Loss and Gain due to scattering process and corresponding delay (adapted with permission from [162]) (b) Intuitive interpretation of the slow light propagation in an EIT medium going from left to right (adapted with permission from [163]).

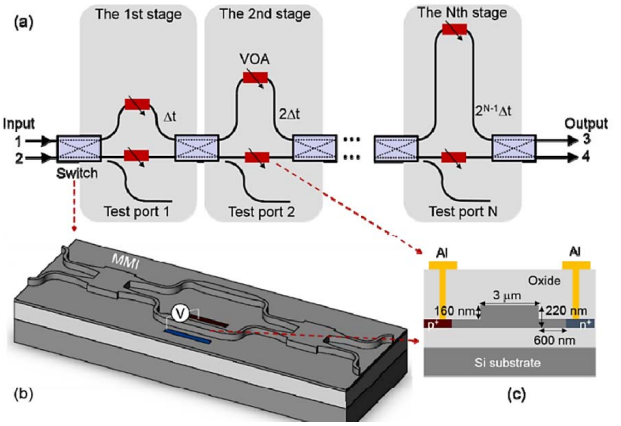

FIGURE 15. (a) Reconfigurable true time delay lines (RTTDL) on SOI platform (b) 3-D view of the single-arm modulated MZI used as an optical switch. (c) Cross-sectional view of the p-i-n diode for optical phase tuning and optical power attenuation. (adapted with permission from [51]).

and showed that by controlling the duty cycles, an average incremental delay of 4.7 ps and a total delay between the first and last waveguides of approximately 181.9 ps can be obtained [160].

D. NONLINEAR PHOTONICS FOR SLOW WAVES

Several research groups demonstrated on-chip slowing down of light utilizing nonlinear photonic schemes i.e., stimulated Raman scattering (SRS), stimulated Brillouin scattering (SBS), four-wave mixing and electromagnetically induced transparency (EIT). In general, any substantial change in frequency-dependent refractive index is associated with a rapid spectral variation in the absorption (or gain) of the material [164]. In SBS, an induced high-frequency acoustic wave modulates refractive index of the medium causing exponential amplification (absorption) of the prove wave causing large change in refractive index due to coupling among pump, probe and downshifted (upshifted) waves [162]. For the case of absorption, corresponding maximum delay occurs at the sides of the resonance peak whereas for gain, the maximum delay coincides with the peak of resonance, depicted in Fig. 14(a). For the SRS, optical phonons are responsible for scattering which is excited vibrational or rotational motion of individual molecules, as opposed to acoustic waves in the SBS process. Another difference is that efficient SBS requires counterpropagating pump-probe geometry whereas SRS can occur in both copropagating and counterpropagating pump-probe structures. Fig. 14(b) depicts an intuitive interpretation of the slow light propagation process in an EIT medium [163].

In 2006, Okawachi *et al.* demonstrated optically tunable on-chip slowing down of light on SOI platform induced by SRS. Within an 8 mm long nanoscale waveguide, the team produced a group-index change of. 15 which generated tunable delays as large as 4 ps for short pulses as short as 3 ps [48]. In addition to being CMOS compatible, it enabled bandwidths exceeding 100 GHz for telecommunication wavelengths. Recently in 2020, Mckay *et al.* demonstrated TTD devices based on SBS. TTD devices based on on-chip SBS offer large delay bandwidth product in addition to simultaneous reconfigurability of carrier frequency and bandwidth, only limited by SBS gain and associated power requirements.They addressed these by combining on-chip silicon nitride MRRs and RF interferometric delay enhancement, and achieved delay tunability over 600 ps over a bandwidth of 1 GHz with enhancement factor of 30 and less than 1 dB of Brillouin gain.

Gaeta's group in 2008 demonstrated another technique to generate large and all-optical delays by using temporal phase conjugation via four-wave mixing in Si nanowaveguide while simultaneously minimizing pulse distortion [165]. They achieved continuously tunable delays over a range of 243 ns for 10 Gb/s non-return-to-zero (NRZ) signals which corresponds to a delay-bandwidth product of 2430. Finally, in 2021, Clementi *et al.* reported observation of EIT and amplification of a weak probe beam in a strongly driven silicon photonic crystal resonator at room temperature based on oscillating temperature field induced in a nonlinear optical cavity [49]. It measured maximum delay of. 41 μs with a FWHM bandwidth of $2\pi \times 17$ MHz, yielding a delay-bandwidth product of 0.45.

E. OTHER SCHEMES AND APPLICATIONS OF TTD

The simplest way to achieve TTD on integrated platform is to physically change the optical path length by routing light through optical waveguides of different length employing optical switches. Even though this approach is not as compact as the approaches based of slow light, it can provide much higher delay-bandwidth product due to low group delay dispersion. Several research groups demonstrated switchable routes on SOI platform to implement TTD devices [51], [52], [166], [167] with maximum of 1.27 ns delay with a 10 ps resolution over a wide wavelength range, reported in [51]. Fig. 15 depicts such a reconfigurable true time delay lines (RTTDL)

on SOI platform. Park *et al.* demonstrated an recirculating buffer utilizing integrated low loss silicon waveguide delay line and a silicon evanescent gate matrix switch with an error free operation at 40 Gb/s data rate with a packet delay of 1.1 ns [168].

The delay lines utilized for beamforming can also be implemented for several other applications. Optical buffer for packet switching routers is another important application of this delay line for data synchronization [169], [170]. Moreover the availability of on-chip tunable delay lines paved the path for integrated microwave photonic signal processors [41], [171]–[173].

IV. CONCLUSION

Modern 5G technology, harnessing the mm-Wave (30-300 GHz) band is poised to usher an era of networking and connectivity with immense possibilities. Beamforming and beam steering are key requirements for mm-Wave systems due to the fundamental limitations of such high frequencies. Traditional phased array antennas are narrow band and conventional beamforming techniques are too bulky, energy hungry, and expensive to integrate into consumer electronics. In this endeavor, we presented a comprehensive review on utilizing slow-wave photonic structures to realize an integrated and wideband true-time-delay (TTD) devices that can operate over the entire mm-Wave band and enable much-needed broadband 5G connectivity using compact beam-forming transceiver architectures. Several on-chip integration techniques are discussed here with their respective challenges and prospects, with focus on SOI integration. The fabrication approaches are completely CMOS compatible, making the process conventional and cheap and will enable future prospect of realizing compact photonic integrated circuits.

REFERENCES

[1] Y. Niu, Y. Li, D. Jin, L. Su, and A. V. Vasilakos, "A survey of millimeter wave communications (mmWave) for 5G: Opportunities and challenges," *Wireless Netw.*, vol. 21, no. 8, pp. 2657–2676, Nov. 2015.

[2] D. I. Lialios, N. Ntetsikas, K. D. Paschaloudis, C. L. Zekios, S. V. Georgakopoulos, and G. A. Kyriacou, "Design of true time delay millimeter wave beamformers for 5G multibeam phased arrays," *Electronics*, vol. 9, no. 8, p. 1331, Aug. 2020.

[3] T. S. Rappaport, Y. Xing, O. Kanhere, S. Ju, A. Madanayake, S. Mandal, A. Alkhateeb, and G. C. Trichopoulos, "Wireless communications and applications above 100 GHz: Opportunities and challenges for 6G and beyond," *IEEE Access*, vol. 7, pp. 78729–78757, 2019.

[4] T. S. Rappaport, S. Sun, R. Mayzus, H. Zhao, Y. Azar, K. Wang, G. N. Wong, J. K. Schulz, M. Samimi, and F. Gutierrez, "Millimeter wave mobile communications for 5G cellular: It will work!" *IEEE Access*, vol. 1, pp. 335–349, 2013.

[5] K. Kibaroglu, M. Sayginer, and G. M. Rebeiz, "A low-cost scalable 32-element 28-GHz phased array transceiver for 5G communication links based on a 2×2 beamformer flip-chip unit cell," *IEEE J. Solid-State Circuits*, vol. 53, no. 5, pp. 1260–1274, Jan. 2018.

[6] B.-H. Ku, P. Schmalenberg, O. Inac, O. D. Gurbuz, J. S. Lee, K. Shiozaki, and M. G. Rebeiz, "A 77–81-GHz 16-element phased-array receiver with ± 50° beam scanning for advanced automotive radars," *IEEE Trans. Microw. Theory Techn.*, vol. 62, no. 11, pp. 2823–2832, Sep. 2014.

[7] G. M. Rebeiz and J. B. Muldavin, "RF MEMS switches and switch circuits," *IEEE Microw. Mag.*, vol. 2, no. 4, pp. 59–71, Dec. 2001.

[8] G. M. Rebeiz, *RF MEMS*. Hoboken, NJ, USA: Wiley, 2004.

[9] S. Han, I. Chih-Lin, Z. Xu, and C. Rowell, "Large-scale antenna systems with hybrid analog and digital beamforming for millimeter wave 5G," *IEEE Commun. Mag.*, vol. 53, no. 1, pp. 186–194, Jan. 2015.

[10] I. Uchendu and J. R. Kelly, "Survey of beam steering techniques available for millimeter wave applications," *Prog. Electromagn. Res. B*, vol. 68, pp. 35–54, 2016.

[11] R. J. Mailloux, *Phased Array Antenna Handbook* (Antennas and Propagation Library), 2nd ed. Boston, MA, USA: Artech House, 2005.

[12] K. Zarb-Adami, A. Faulkner, J. G. B. de Vaate, G. W. Kant, and P. Picard, "Beamforming techniques for large-N aperture arrays," in *Proc. IEEE Int. Symp. Phased Array Syst. Technol. (ARRAY)*, Waltham, MA, USA, Oct. 2010, pp. 883–890.

[13] R. L. Haupt, "Antenna arrays in the time domain: An introduction to timed arrays," *IEEE Antennas Propag. Mag.*, vol. 59, no. 3, pp. 33–41, Jun. 2017.

[14] M. Longbrake, "True time-delay beamsteering for radar," in *Proc. IEEE Nat. Aerosp. Electron. Conf. (NAECON)*, Dayton, OH, USA, Jul. 2012, pp. 246–249.

[15] Y. Liu, J. Yao, and J. Yang, "Wideband true-time-delay unit for phased array beamforming using discrete-chirped fiber grating prism," *Opt. Commun.*, vol. 207, nos. 1–6, pp. 177–187, Jun. 2002.

[16] Y. Jiang, B. Howley, Z. Shi, Q. Zhou, R. T. Chen, M. Y. Chen, G. Brost, and C. Lee, "Dispersion-enhanced photonic crystal fiber array for a true time-delay structured X-band phased array antenna," *IEEE Photon. Technol. Lett.*, vol. 17, no. 1, pp. 187–189, Jan. 1, 2005.

[17] Y. Chen and Y. Chen, "A fully packaged true time delay module for a K-band phased array antenna system demonstration," *IEEE Photon. Technol. Lett.*, vol. 14, no. 8, pp. 1175–1177, Aug. 2002.

[18] L. Zhang, M. Li, N. Shi, X. Zhu, S. Sun, J. Tang, W. Li, and N. Zhu, "Photonic true time delay beamforming technique with ultra-fast beam scanning," *Opt. Exp.*, vol. 25, no. 13, p. 14524, Jun. 2017.

[19] N. K. Nahar and R. G. Rojas, "Low-loss polynomial white cell optical true-time delay engine for wideband radio frequency array beam steering," *Appl. Opt.*, vol. 48, no. 20, p. 3921, Jul. 2009.

[20] N. K. Nahar, B. Raines, R. G. Rojas, and B. Strojny, "Wideband antenna array beam steering with free-space optical true-time delay engine," *IET Microw., Antennas Propag.*, vol. 5, no. 6, p. 740, 2011.

[21] R. Higgins, N. K. Nahar, and B. L. Anderson, "Design and demonstration of a switching engine for a binary true-time-delay device that uses a white cell," *Appl. Opt.*, vol. 42, no. 23, p. 4747, Aug. 2003.

[22] J. Yang, Y. Liu, S. C. Tjin, and N. Q. Ngo, "Tunable chirped fiber grating based variable time-delay network for phased-array antenna beamforming," *Int. J. Infr. Millim. Waves*, vol. 24, pp. 593–601, Apr. 2003.

[23] J. Zhang and J. Yao, "Broadband microwave signal processing based on photonic dispersive delay lines," *IEEE Trans. Microw. Theory Techn.*, vol. 65, no. 5, pp. 1891–1903, May 2017.

[24] Z. Shi and R. W. Boyd, "Discretely tunable optical packet delays using channelized slow light," *Phys. Rev. A, Gen. Phys.* vol. 79, no. 1, Jan. 2009, Art. no. 013805.

[25] C. Yu, T. Luo, L. Zhang, and A. E. Willner, "Data pulse distortion induced by a slow-light tunable delay line in optical fiber," *Opt. Lett.*, vol. 32, no. 1, p. 20, Jan. 2007.

[26] J. E. Sharping, Y. Okawachi, and A. L. Gaeta, "Wide bandwidth slow light using a Raman fiber amplifier," *Opt. Exp.*, vol. 13, no. 16, p. 6092, 2005.

[27] K. Lee and N. M. Lawandy, "Optically induced pulse delay in a solid-state Raman amplifier," *Appl. Phys. Lett.*, vol. 78, no. 6, pp. 703–705, Feb. 2001.

[28] X. Yi, T. X. H. Huang, and R. A. Minasian, "Photonic beamforming based on programmable phase shifters with amplitude and phase control," *IEEE Photon. Technol. Lett.*, vol. 23, no. 18, pp. 1286–1288, Sep. 15, 2011.

[29] M. Burla, L. R. Cortés, M. Li, X. Wang, L. Chrostowski, and J. Azaña, "Integrated waveguide Bragg gratings for microwave photonics signal processing," *Opt. Exp.*, vol. 21, no. 21, p. 25120, Oct. 2013.

[30] I. Giuntoni, D. Stolarek, D. I. Kroushkov, J. Bruns, L. Zimmermann, B. Tillack, and K. Petermann, "Continuously tunable delay line based on SOI tapered Bragg gratings," *Opt. Exp.*, vol. 20, no. 10, p. 11241, May 2012.

[31] J. Cardenas, M. A. Foster, N. Sherwood-Droz, C. B. Poitras, H. L. R. Lira, B. Zhang, A. L. Gaeta, J. B. Khurgin, P. Morton, and M. Lipson, "Wide-bandwidth continuously tunable optical delay line using silicon microring resonators," *Opt. Exp.*, vol. 18, no. 25, p. 26525, Dec. 2010.

[32] M. Burla, D. Marpaung, L. Zhuang, A. Leinse, M. Hoekman, R. Heideman, and C. Roeloffzen, "Integrated photonic Ku-band beamformer chip with continuous amplitude and delay control," *IEEE Photon. Technol. Lett.*, vol. 25, no. 12, pp. 1145–1148, Jun. 15, 2013.

[33] C. Xiang, M. L. Davenport, J. B. Khurgin, P. A. Morton, and J. E. Bowers, "Low-loss continuously tunable optical true time delay based on Si3N4 ring resonators," *IEEE J. Sel. Topics Quantum Electron.*, vol. 24, no. 4, pp. 1–9, Jul. 2018.

[34] L. Zhuang, C. G. H. Roeloffzen, R. G. Heideman, A. Borreman, A. Meijerink, and W. van Etten, "Single-chip ring resonator-based 1×8 optical beam forming network in CMOS-compatible waveguide technology," *IEEE Photon. Technol. Lett.*, vol. 19, no. 15, pp. 1130–1132, Aug. 15, 2007.

[35] A. Meijerink, C. G. H. Roeloffzen, R. Meijerink, L. Zhuang, D. A. I. Marpaung, M. J. Bentum, M. Burla, J. Verpoorte, P. Jorna, A. Hulzinga, and W. van Etten, "Novel ring resonator-based integrated photonic beamformer for broadband phased array receive antennas—Part I: Design and performance analysis," *J. Lightw. Technol.*, vol. 28, no. 1, pp. 3–18, Jan. 15, 2010.

[36] L. Zhuang, C. G. H. Roeloffzen, A. Meijerink, M. Burla, D. Marpaung, A. Leinse, M. Hoekman, R. G. Heideman, and W. van Etten, "Novel ring resonator-based integrated photonic beamformer for broadband phased array receive antennas—Part II: Experimental prototype," *J. Lightw. Technol.*, vol. 28, no. 1, pp. 19–31, Jan. 15, 2010.

[37] Y. Liu, A. Wichman, B. Isaac, J. Kalkavage, E. J. Adles, T. R. Clark, and J. Klamkin, "Tuning optimization of ring resonator delays for integrated optical beam forming networks," *J. Lightw. Technol*, vol. 35, no. 22, pp. 4954–4960, Nov. 15, 2017.

[38] Y. Liu, A. R. Wichman, B. Isaac, J. Kalkavage, E. J. Adles, and J. Klamkin, "Ultra-low-loss silicon nitride optical beamforming network for wideband wireless applications," *IEEE J. Sel. Topics Quantum Electron.*, vol. 24, no. 4, p. 10, Apr. 2018.

[39] N. M. Tessema, Z. Cao, J. H. C. Van Zantvoort, K. A. Mekonnen, A. Dubok, E. Tangdiongga, A. B. Smolders, and A. M. J. Koonen, "A tunable Si_3N_4 integrated true time delay circuit for optically-controlled K-band radio beamformer in satellite communication," *J. Lightw. Technol.*, vol. 34, no. 20, pp. 4736–4743, Oct. 15, 2016.

[40] G. Choo, C. K. Madsen, S. Palermo, and K. Entesari, "Automatic monitor-based tuning of an RF silicon photonic 1×4 asymmetric binary tree true-time-delay beamforming network," *J. Lightw. Technol.*, vol. 36, no. 22, pp. 5263–5275, Nov. 15, 2018.

[41] J. Sancho, J. Bourderionnet, J. Lloret, S. Combrié, I. Gasulla, S. Xavier, S. Sales, P. Colman, G. Lehoucq, D. Dolfi, J. Capmany, and A. De Rossi, "Integrable microwave filter based on a photonic crystal delay line," *Nature Commun.*, vol. 3, no. 1, p. 1075, Jan. 2012.

[42] H. Gersen, T. J. Karle, R. J. P. Engelen, W. Bogaerts, J. P. Korterik, N. F. van Hulst, T. F. Krauss, and L. Kuipers, "Real-space observation of ultraslow light in photonic crystal waveguides," *Phys. Rev. Lett.*, vol. 94, no. 7, Feb. 2005, Art. no. 073903.

[43] Y. A. Vlasov, M. O'Boyle, H. F. Hamann, and S. J. McNab, "Active control of slow light on a chip with photonic crystal waveguides," *Nature*, vol. 438, no. 7064, pp. 65–69, Nov. 2005.

[44] D. O'Brien, A. Gomez-Iglesias, M. D. Settle, A. Michaeli, M. Salib, and T. F. Krauss, "Tunable optical delay using photonic crystal heterostructure nanocavities," *Phys. Rev. B, Condens. Matter*, vol. 76, no. 11, Sep. 2007, Art. no. 115110.

[45] B. Paul, N. K. Nahar, and K. Sertel, "Harnessing the frozen-mode in coupled silicon ridge waveguides for true time delay applications," in *Proc. Int. Conf. Electromagn. Adv. Appl. (ICEAA)*, Granada, Spain, Sep. 2019, p. 0552.

[46] M. L. Povinelli, S. G. Johnson, and J. D. Joannopoulos, "Slow-light, band-edge waveguides for tunable time delays," *Opt. Exp.*, vol. 13, no. 18, p. 7145, 2005.

[47] J. E. Heebner and R. W. Boyd, "Slow and stopped light 'slow' and 'fast' light in resonator-coupled waveguides," *J. Modern Opt.*, vol. 49, nos. 14–15, pp. 2629–2636, Nov. 2002.

[48] Y. Okawachi, M. Foster, J. Sharping, A. Gaeta, Q. Xu, and M. Lipson, "All-optical slow-light on a photonic chip," *Opt. Exp.*, vol. 14, no. 6, p. 2317, 2006.

[49] M. Clementi, S. Iadanza, S. A. Schulz, G. Urbinati, D. Gerace, L. O'Faloain, and M. Galli, "Thermo-optically induced transparency on a photonic chip," *Light, Sci. Appl.*, vol. 10, no. 1, p. 240, Dec. 2021.

[50] X. Xue, Y. Xuan, C. Bao, S. Li, X. Zheng, B. Zhou, M. Qi, and A. M. Weiner, "Microcomb-based true-time-delay network for microwave beamforming with arbitrary beam pattern control," *J. Lightw. Technol.*, vol. 36, no. 12, pp. 2312–2321, Jun. 15, 2018.

[51] J. Xie, L. Zhou, Z. Li, J. Wang, and J. Chen, "Seven-bit reconfigurable optical true time delay line based on silicon integration," *Opt. Exp.*, vol. 22, no. 19, p. 22707, Sep. 2014.

[52] X. Wang, L. Zhou, R. Li, J. Xie, L. Lu, K. Wu, and J. Chen, "Continuously tunable ultra-thin silicon waveguide optical delay line," *Optica*, vol. 4, no. 5, p. 507, May 2017.

[53] Q. Q. Song, Z. F. Hu, and K. X. Chen, "Scalable and reconfigurable true time delay line based on an ultra-low-loss silica waveguide," *Appl. Opt.*, vol. 57, no. 16, p. 4434, Jun. 2018.

[54] Q. Xu, B. Shmidt, S. Pradhan, and M. Lipson, "Micrometre-scale silicon electro-optic modulator," *Nature*, vol. 435, no. 7040, pp. 325–327, May 2005.

[55] G. Lenz, B. J. Eggleton, C. K. Madsen, and R. E. Slusher, "Optical delay lines based on optical filters," *IEEE J. Quantum Electron.*, vol. 37, no. 4, pp. 525–532, Apr. 2001.

[56] L. Chrostowski and M. Hochberg, *Silicon Photonics Design*. Cambridge, U.K.: Cambridge Univ. Press, 2015.

[57] S. Shekhar, "Silicon photonics: A brief tutorial," *IEEE Solid State Circuits Mag.*, vol. 13, no. 3, pp. 22–32, Aug. 2021.

[58] J. Chen, B. Paul, and A. C. Coleman, "Tunable repetition rates in compound cavity mode locked laser diodes using external reflector," in *Proc. Conf. Lasers Electro-Optics (CLEO)*, 2020, pp. 1–2.

[59] K. Sun and A. Beling, "High-speed photodetectors for microwave photonics," *Appl. Sci.*, vol. 9, no. 4, p. 623, Feb. 2019.

[60] R. Rotman, M. Tur, and L. Yaron, "True time delay in phased arrays," *Proc. IEEE*, vol. 104, no. 3, pp. 504–518, Mar. 2016.

[61] W. Ng, A. A. Walston, G. L. Tangonan, J. J. Lee, I. L. Newberg, and N. Bernstein, "The first demonstration of an optically steered microwave phased array antenna using true-time-delay," *J. Lightw. Technol.*, vol. 9, no. 9, pp. 1124–1131, Sep. 15, 1991.

[62] I. Frigyes and A. J. Seeds, "Optically generated true-time delay in phased-array antennas," *IEEE Trans. Microw. Theory Techn.*, vol. 43, no. 9, pp. 2378–2386, Sep. 1995.

[63] A. Figotin and I. Vitebskiy, "Slow light in photonic crystals," *Waves Random Complex Media*, vol. 16, no. 3, pp. 293–382, Aug. 2006.

[64] L. V. Hau, S. E. Harris, Z. Dutton, and C. H. Behroozi, "Light speed reduction to 17 metres per second in an ultracold atomic gas," *Nature*, vol. 397, no. 6720, pp. 594–598, Feb. 1999.

[65] R. S. Tucker, P.-C. Ku, and C. J. Chang-Hasnain, "Slow-light optical buffers: Capabilities and fundamental limitations," *J. Lightw. Technol.*, vol. 23, no. 12, pp. 4046–4066, Dec. 15, 2005.

[66] M. Notomi, "Manipulating light by photonic crystals," *NTT Tech. Rev.*, vol. 7, no. 9, p. 10, 2009.

[67] T. Baba, T. Kawaaski, H. Sasaki, J. Adachi, and D. Mori, "Large delay-bandwidth product and tuning of slow light pulse in photonic crystal coupled waveguide," *Opt. Exp.*, vol. 16, no. 12, p. 9245, Jun. 2008.

[68] E. Yablonovitch, "Inhibited spontaneous emission in solid-state physics and electronics," *Phys. Rev. Lett.*, vol. 58, no. 20, pp. 2059–2062, May 1987.

[69] S. John, "Strong localization of photons in certain disordered dielectric superlattices," *Phys. Rev. Lett.*, vol. 58, pp. 2486–2489, Jun. 1987.

[70] T. F. Krauss, R. M. D. L. Rue, and S. Brand, "Two-dimensional photonic-bandgap structures operating at near-infrared wavelengths," *Nature*, vol. 383, no. 6602, pp. 699–702, Oct. 1996.

[71] T. Baba, A. Motegi, T. Iwai, N. Fukaya, Y. Watanabe, and A. Sakai, "Light propagation characteristics of straight single-line-defect waveguides in photonic crystal slabs fabricated into a silicon-on-insulator substrate," *IEEE J. Quantum Electron.*, vol. 38, no. 7, pp. 743–752, Jul. 2002.

[72] D. O'Brien, M. D. Settle, T. Karle, A. Michaeli, M. Salib, and T. F. Krauss, "Coupled photonic crystal heterostructure nanocavities," *Opt. Exp.*, vol. 15, no. 3, p. 1228, 2007.

[73] S.-C. Huang, M. Kato, E. Kuramochi, C.-P. Lee, and M. Notomi, "Time-domain and spectral-domain investigation of inflection-point slow-light modes in photonic crystal coupled waveguides," *Opt. Exp.*, vol. 15, no. 6, p. 3543, 2007.

[74] K. Üstün and H. Kurt, "Ultra slow light achievement in photonic crystals by merging coupled cavities with waveguides," *Opt. Exp.*, vol. 18, no. 20, p. 21155, Sep. 2010.

[75] A. Chutinan and S. Noda, "Waveguides and waveguide bends in two-dimensional photonic crystal slabs," *Phys. Rev. B, Condens. Matter*, vol. 62, pp. 4488–4492, Aug. 2000.
[76] J. D. Joannopoulos, P. R. Villeneuve, and S. Fan, "Photonic crystals: Putting a new twist on light," *Nature*, vol. 386, no. 6621, pp. 143–149, Mar. 1997.
[77] A. Mekis, J. C. Chen, I. Kurland, S. Fan, P. R. Villeneuve, and J. D. Joannopoulos, "High transmission through sharp bends in photonic crystal waveguides," *Phys. Rev. Lett.*, vol. 77, no. 18, pp. 3787–3790, Oct. 1996.
[78] T. F. Krauss, "Slow light in photonic crystal waveguides," *J. Phys. D, Appl. Phys.*, vol. 40, no. 9, pp. 2666–2670, May 2007.
[79] L. H. Frandsen, A. V. Lavrinenko, J. Fage-Pedersen, and P. I. Borel, "Photonic crystal waveguides with semi-slow light and tailored dispersion properties," *Opt. Exp.*, vol. 14, no. 20, p. 9444, 2006.
[80] A. Y. Petrov and M. Eich, "Zero dispersion at small group velocities in photonic crystal waveguides," *Appl. Phys. Lett.*, vol. 85, no. 21, pp. 4866–4868, Nov. 2004.
[81] R. Engelen, Y. Sugimoto, Y. Watanabe, J. Korterik, N. Ikeda, N. van Hulst, K. Asakawa, and L. Kuipers, "The effect of higher-order dispersion on slow light propagation in photonic crystal waveguides," *Opt. Exp.*, vol. 14, no. 4, pp. 1658–1672, Feb. 2006.
[82] J. Li, T. P. White, L. O'Faolain, A. Gomez-Iglesias, and T. F. Krauss, "Systematic design of flat band slow light in photonic crystal waveguides," *Opt. Exp.*, vol. 16, no. 9, p. 6227, Apr. 2008.
[83] D. Mori and T. Baba, "Dispersion-controlled optical group delay device by chirped photonic crystal waveguides," *Appl. Phys. Lett.*, vol. 85, no. 7, pp. 1101–1103, Aug. 2004.
[84] D. Mori and T. Baba, "Wideband and low dispersion slow light by chirped photonic crystal coupled waveguide," *Opt. Exp.*, vol. 13, no. 23, p. 9398, Nov. 2005.
[85] D. Mori, S. Kubo, H. Sasaki, and T. Baba, "Experimental demonstration of wideband dispersion-compensated slow light by a chirped photonic crystal directional coupler," *Opt. Exp.*, vol. 15, no. 9, p. 5264, 2007.
[86] T. Kawasaki, D. Mori, and T. Baba, "Experimental observation of slow light in photonic crystal coupled waveguides," *Opt. Exp.*, vol. 15, no. 16, p. 10274, 2007.
[87] M. D. Settle, R. J. P. Engelen, M. Salib, A. Michaeli, L. Kuipers, and T. F. Krauss, "Flatband slow light in photonic crystals featuring spatial pulse compression and terahertz bandwidth," *Opt. Exp.*, vol. 15, no. 1, p. 219, 2007.
[88] S. Kubo, D. Mori, and T. Baba, "Low-group-velocity and low-dispersion slow light in photonic crystal waveguides," *Opt. Lett.*, vol. 32, no. 20, p. 2981, Oct. 2007.
[89] Y. Hamachi, S. Kubo, and T. Baba, "Slow light with low dispersion and nonlinear enhancement in a lattice-shifted photonic crystal waveguide," *Opt. Lett.*, vol. 34, no. 7, p. 1072, Apr. 2009.
[90] M. Notomi, K. Yamada, A. Shinya, J. Takahashi, C. Takahashi, and I. Yokohama, "Extremely large group-velocity dispersion of line-defect waveguides in photonic crystal slabs," *Phys. Rev. Lett.*, vol. 87, no. 25, p. 253902, Nov. 2001.
[91] M. Lončar, D. Nedeljković, T. Doll, J. Vučković, A. Scherer, and T. P. Pearsall, "Waveguiding in planar photonic crystals," *Appl. Phys. Lett.*, vol. 77, no. 13, pp. 1937–1939, Sep. 2000.
[92] M. Notomi, A. Shinya, S. Mitsugi, E. Kuramochi, and H.-Y. Ryu, "Waveguides, resonators and their coupled elements in photonic crystal slabs," *Opt. Exp.*, vol. 12, no. 8, p. 1551, 2004.
[93] S. Nishikawa, S. Lan, N. Ikeda, Y. Sugimoto, H. Ishikawa, and K. Asakawa, "Optical characterization of photonic crystal delay lines based on one-dimensional coupled defects," *Opt. Lett.*, vol. 27, no. 23, p. 2079, Dec. 2002.
[94] Y. Sugimoto, S. Lan, S. Nishikawa, N. Ikeda, H. Ishikawa, and K. Asakawa, "Design and fabrication of impurity band-based photonic crystal waveguides for optical delay lines," *Appl. Phys. Lett.*, vol. 81, no. 11, pp. 1946–1948, Sep. 2002.
[95] M. Notomi, T. Tanabe, A. Shinya, E. Kuramochi, H. Taniyama, S. Mitsugi, and M. Morita, "Nonlinear and adiabatic control of high-Q photonic crystal nanocavities," *Opt. Exp.*, vol. 15, no. 26, p. 17458, 2007.
[96] M. Notomi, E. Kuramochi, and T. Tanabe, "Large-scale arrays of ultrahigh-Q coupled nanocavities," *Nature Photon.*, vol. 2, no. 12, pp. 741–747, Dec. 2008.
[97] N. Ishikura, T. Baba, E. Kuramochi, and M. Notomi, "Large tunable fractional delay of slow light pulse and its application to fast optical correlator," *Opt. Exp.*, vol. 19, no. 24, p. 24102, Nov. 2011.
[98] N. Ishikura, R. Hosoi, R. Hayakawa, T. Tamanuki, M. Shinkawa, and T. Baba, "Photonic crystal tunable slow light device integrated with multi-heaters," *Appl. Phys. Lett.*, vol. 100, no. 22, May 2012, Art. no. 221110.
[99] B. Paul, N. K. Nahar, and K. Sertel, "Frozen mode in coupled silicon ridge waveguides for optical true time delay applications," *J. Opt. Soc. Amer. B, Opt. Phys.*, vol. 38, no. 5, p. 1435, May 2021.
[100] A. Figotin and I. Vitebskiy, "Slow wave phenomena in photonic crystals," *Laser Photon. Rev.*, vol. 5, no. 2, pp. 201–213, Mar. 2011.
[101] R. Almhmadi and K. Sertel, "Frozen-light modes in 3-way coupled silicon ridge waveguides," in *Proc. USA Nat. Committee URSI Nat. Radio Sci. Meeting (USNC-URSI NRSM)*, Boulder, CO, USA, Jan. 2019, pp. 1–2.
[102] N. Apaydin, L. Zhang, K. Sertel, and J. L. Volakis, "Experimental verification of frozen mode phenomenon in printed magnetic photonic crystals," in *Proc. 5th Eur. Conf. Antennas Propag. (EUCAP)*, Apr. 2011, pp. 2396–2398.
[103] J. L. Volakis and K. Sertel, "Narrowband and wideband metamaterial antennas based on degenerate band edge and magnetic photonic crystals," *Proc. IEEE*, vol. 99, no. 10, pp. 1732–1745, Oct. 2011.
[104] K. Sertel and J. L. Volakis, "Emulation of anisotropic media in transmission line," U.S. Patent 8 384 493, Feb. 26, 2013.
[105] M. B. Stephanson, K. Sertel, and J. L. Volakis, "Frozen modes in coupled microstrip lines printed on ferromagnetic substrates," *IEEE Microw. Wireless Compon. Lett.*, vol. 18, no. 5, pp. 305–307, May 2008.
[106] N. Apaydin, K. Sertel, and J. L. Volakis, "Nonreciprocal leaky-wave antenna based on coupled microstrip lines on a non-uniformly biased ferrite substrate," *IEEE Trans. Antennas Propag.*, vol. 61, no. 7, pp. 3458–3465, Jul. 2013.
[107] N. Apaydin, K. Sertel, and J. L. Volakis, "Nonreciprocal and magnetically scanned leaky-wave antenna using coupled CRLH lines," *IEEE Trans. Antennas Propag.*, vol. 62, no. 6, pp. 2954–2961, Jun. 2014.
[108] G. Mumcu, K. Sertel, and J. L. Volakis, "Miniature antenna using printed coupled lines emulating degenerate band edge crystals," *IEEE Trans. Antennas Propag.*, vol. 57, no. 6, pp. 1618–1624, Jun. 2009.
[109] J. R. Burr, N. Gutman, C. M. de Sterke, I. Vitebskiy, and R. M. Reano, "Degenerate band edge resonances in coupled periodic silicon optical waveguides," *Opt. Exp.*, vol. 21, no. 7, pp. 8736–8745, Apr. 2013.
[110] M. G. Wood, J. R. Burr, and R. M. Reano, "Degenerate band edge resonances in periodic silicon ridge waveguides," *Opt. Lett.*, vol. 40, no. 11, pp. 2493–2496, Jun. 2015.
[111] J. B. Khurgin, "Expanding the bandwidth of slow-light photonic devices based on coupled resonators," *Opt. Lett.*, vol. 30, no. 5, p. 513, Mar. 2005.
[112] A. Melloni, F. Morichetti, and M. Martinelli, "Linear and nonlinear pulse propagation in coupled resonator slow-wave optical structures," *Opt. Quantum Electron.*, vol. 35, no. 4/5, pp. 365–379, Mar. 2003.
[113] H. F. Taylor, "Enhanced electrooptic modulation efficiency utilizing slow-wave optical propagation," *J. Lightw. Technol.*, vol. 17, no. 10, pp. 1875–1883, Oct. 15, 1999.
[114] A. Yariv, Y. Xu, R. K. Lee, and A. Scherer, "Coupled-resonator optical waveguide: A proposal and analysis," *Optics Lett.*, vol. 24, no. 11, p. 711, Jun. 1999.
[115] J. K. S. Poon, J. Scheuer, Y. Xu, and A. Yariv, "Designing coupled-resonator optical waveguide delay lines," *J. Opt. Soc. Amer. B, Opt. Phys.*, vol. 21, no. 9, p. 1665, Sep. 2004.
[116] J. E. Heebner, R. W. Boyd, and Q.-H. Park, "Slow light, induced dispersion, enhanced nonlinearity, and optical solitons in a resonator-array waveguide," *Phys. Rev. E, Stat. Phys. Plasmas Fluids Relat. Interdiscip. Top.*, vol. 65, no. 3, Mar. 2002, Art. no. 036619.
[117] F. Morichetti, C. Ferrari, A. Canciamilla, and A. Melloni, "The first decade of coupled resonator optical waveguides: Bringing slow light to applications," *Laser Photon. Rev.*, vol. 6, no. 1, pp. 74–96, Jan. 2012.
[118] Q. Xu, J. Shakya, and M. Lipson, "Direct measurement of tunable optical delays on chip analogue to electromagnetically induced transparency," *Opt. Exp.*, vol. 14, no. 14, p. 6463, 2006.
[119] B. Z. Steinberg, A. Boag, and R. Lisitsin, "Sensitivity analysis of narrowband photonic crystal filters and waveguides to structure variations and inaccuracy," *J. Opt. Soc. Amer. A, Opt. Image Sci.*, vol. 20, no. 1, pp. 138–146, Jan. 2003.
[120] S. Mookherjea and A. Oh, "Effect of disorder on slow light velocity in optical slow-wave structures," *Opt. Lett.*, vol. 32, no. 3, p. 289, Feb. 2007.

[121] A. Melloni, A. Canciamilla, C. Ferrari, F. Morichetti, L. O'Faolain, T. Krauss, R. De La Rue, A. Samarelli, and M. Sorel, "Tunable delay lines in silicon photonics: Coupled resonators and photonic crystals, a comparison," *IEEE Photon. J.*, vol. 2, no. 2, pp. 181–194, Apr. 2010.

[122] J. Poon, J. Scheuer, S. Mookherjea, G. T. Paloczi, Y. Huang, and A. Yariv, "Matrix analysis of microring coupled-resonator optical waveguides," *Opt. Exp.*, vol. 12, no. 1, p. 90, 2004.

[123] S. Mookherjea and A. Yariv, "Coupled resonator optical waveguides," *IEEE J. Sel. Topics Quantum Electron.*, vol. 8, no. 3, pp. 448–456, May 2002.

[124] F. Morichetti, A. Melloni, A. Breda, A. Canciamilla, C. Ferrari, and M. Martinelli, "A reconfigurable architecture for continuously variable optical slow-wave delay lines," *Opt. Exp.*, vol. 15, no. 25, p. 17273, 2007.

[125] F. Morichetti, A. Melloni, C. Ferrari, and M. Martinelli, "Error-free continuously-tunable delay at 10 Gbit/s in a reconfigurable on-chip delay-line," *Opt. Exp.*, vol. 16, no. 12, p. 8395, Jun. 2008.

[126] A. Melloni, F. Morichetti, C. Ferrari, and M. Martinelli, "Continuously tunable 1 byte delay in coupled-resonator optical waveguides," *Opt. Lett.*, vol. 33, no. 20, p. 2389, Oct. 2008.

[127] J. K. S. Poon, L. Zhu, G. A. DeRose, and A. Yariv, "Polymer microring coupled-resonator optical waveguides," *J. Lightw. Technol.*, vol. 24, no. 4, pp. 1843–1849, Apr. 15, 2006.

[128] B. Little, S. Chu, P. Absil, J. Hryniewicz, F. Johnson, F. Seiferth, D. Gill, V. Van, O. King, and M. Trakalo, "Very high-order microring resonator filters for WDM applications," *IEEE Photon. Technol. Lett.*, vol. 16, no. 10, pp. 2263–2265, Oct. 2004.

[129] Y. Vlasov, W. M. J. Green, and F. Xia, "High-throughput silicon nanophotonic wavelength-insensitive switch for on-chip optical networks," *Nature Photon.*, vol. 2, no. 4, pp. 242–246, Apr. 2008.

[130] F. Xia, L. Sekaric, and Y. Vlasov, "Ultracompact optical buffers on a silicon chip," *Nature Photon.*, vol. 1, no. 1, pp. 65–71, Jan. 2007.

[131] A. Canciamilla, M. Torregiani, C. Ferrari, F. Morichetti, R. M. De La Rue, A. Samarelli, M. Sorel, and A. Melloni, "Silicon coupled-ring resonator structures for slow light applications: Potential, impairments and ultimate limits," *J. Opt.*, vol. 12, no. 10, Oct. 2010, Art. no. 104008.

[132] F. Xia, L. Sekaric, M. O'Boyle, and Y. Vlasov, "Coupled resonator optical waveguides based on silicon-on-insulator photonic wires," *Appl. Phys. Lett.*, vol. 89, no. 4, Jul. 2006, Art. no. 041122.

[133] F. Xia, M. Rooks, L. Sekaric, and Y. Vlasov, "Ultra-compact high order ring resonator filters using submicron silicon photonic wires for on-chip optical interconnects," *Opt. Exp.*, vol. 15, no. 19, p. 11934, 2007.

[134] J. Komma, C. Schwarz, G. Hofmann, D. Heinert, and R. Nawrodt, "Thermo-optic coefficient of silicon at 1550 nm and cryogenic temperatures," *Appl. Phys. Lett.*, vol. 101, no. 4, Jul. 2012, Art. no. 041905.

[135] F. Gan, T. Barwicz, M. A. Popovic, M. S. Dahlem, C. W. Holzwarth, P. T. Rakich, H. I. Smith, E. P. Ippen, and F. X. Kartner, "Maximizing the thermo-optic tuning range of silicon photonic structures," in *Proc. Photon. Switching*, Aug. 2007, pp. 67–68.

[136] M. S. Dahlem, C. W. Holzwarth, A. Khilo, F. X. Kärtner, H. I. Smith, and P. E. Ippen, "Reconfigurable multi-channel second-order silicon microring-resonator filterbanks for on-chip WDM systems," *Opt. Exp.*, vol. 19, no. 1, pp. 306–316, Jan. 2011.

[137] F. Morichetti, A. Melloni, C. Ferrari, and M. Martinelli, "Error-free continuously-tunable delay at 10 Gbit/s in a reconfigurable on-chip delay-line," *Opt. Exp.*, vol. 16, no. 12, p. 8395, Jun. 2008.

[138] F. Morichetti, A. Melloni, C. Canavesi, F. Persia, M. Martinelli, and M. Sorel, "Tunable slow-wave optical delay lines," in *Slow Fast Light, Tech. Dig. (CD)*. Optica Publishing Group, 2006, Paper MB2.

[139] M. L. Cooper, G. Gupta, M. A. Schneider, W. M. J. Green, S. Assefa, F. Xia, Y. A. Vlasov, and S. Mookherjea, "Statistics of light transport in 235-ring silicon coupled-resonator optical waveguides," *OSA Opt. Exp.*, vol. 18, no. 25, pp. 26505–26516, Dec. 2010.

[140] M. Y. Nada, M. A. K. Othman, and F. Capolino, "Theory of coupled resonator optical waveguides exhibiting high-order exceptional points of degeneracy," *Phys. Rev. B, Condens. Matter*, vol. 96, no. 18, Nov. 2017, Art. no. 184304.

[141] A. Herrero-Parareda, I. Vitebskiy, J. Scheuer, and F. Capolino, "Frozen mode in an asymmetric serpentine optical waveguide," *Adv. Photon. Res.*, May 2022, Art. no. 2100377.

[142] J. E. Heebner, R. W. Boyd, and Q.-H. Park, "SCISSOR solitons and other novel propagation effects in microresonator-modified waveguides," *J. Opt. Soc. Amer. B, Opt. Phys.*, vol. 19, no. 4, p. 722, Apr. 2002.

[143] J. B. Khurgin and P. A. Morton, "Tunable wideband optical delay line based on balanced coupled resonator structures," *Opt. Lett.*, vol. 34, no. 17, p. 2655, Sep. 2009.

[144] P. A. Morton, J. Cardenas, J. B. Khurgin, and M. Lipson, "Fast thermal switching of wideband optical delay line with no long-term transient," *IEEE Photon. Technol. Lett.*, vol. 24, no. 6, pp. 512–514, Mar. 15, 2012.

[145] J. Xie, L. Zhou, Z. Zou, J. Wang, X. Li, and J. Chen, "Continuously tunable reflective-type optical delay lines using microring resonators," *Opt. Exp.*, vol. 22, no. 1, p. 817, Jan. 2014.

[146] M. Y. Nada and F. Capolino, "Exceptional point of sixth-order degeneracy in a modified coupled-resonator optical waveguide," *J. Opt. Soc. Amer. B, Opt. Phys.*, vol. 37, no. 8, p. 2319, Aug. 2020.

[147] S. Khan, M. A. Baghban, and S. Fathpour, "Electronically tunable silicon photonic delay lines," *Opt. Exp.*, vol. 19, no. 12, pp. 11780–11785, 2011.

[148] W. Zhang and J. Yao, "A fully reconfigurable waveguide Bragg grating for programmable photonic signal processing," *Nature Commun.*, vol. 9, no. 1, p. 1396, Dec. 2018.

[149] K. O. Hill, Y. Fujii, D. C. Johnson, and B. S. Kawasaki, "Photosensitivity in optical fiber waveguides: Application to reflection filter fabrication," *Appl. Phys. Lett.*, vol. 32, no. 10, pp. 647–649, May 1978.

[150] T. E. Murphy, J. T. Hastings, and H. I. Smith, "Fabrication and characterization of narrow-band Bragg-reflection filters in silicon-on-insulator ridge waveguides," *J. Lightw. Technol.*, vol. 19, no. 12, pp. 1938–1942, Dec. 15, 2001.

[151] S. Khan and S. Fathpour, "Demonstration of tunable optical delay lines based on apodized grating waveguides," *Opt. Exp.*, vol. 21, no. 17, p. 19538, Aug. 2013.

[152] S. Khan and S. Fathpour, "Demonstration of complementary apodized cascaded grating waveguides for tunable optical delay lines," *Opt. Lett.*, vol. 38, no. 19, p. 3914, Oct. 2013.

[153] W. Shi, V. Veerasubramanian, D. Patel, and D. V. Plant, "Tunable nanophotonic delay lines using linearly chirped contradirectional couplers with uniform Bragg gratings," *Opt. Lett.*, vol. 39, no. 3, p. 701, Feb. 2014.

[154] F. Zhang, J. Dong, Y. Zhu, X. Gao, and X. Zhang, "Integrated optical true time delay network based on grating-assisted contradirectional couplers for phased array antennas," *IEEE J. Sel. Topics Quantum Electron.*, vol. 26, no. 5, pp. 1–7, Sep. 2020.

[155] P. J. Bock, P. Cheben, J. H. Schmid, J. Lapointe, A. Deâge, D.-X. Xu, S. Janz, A. Densmore, and T. J. Hall, "Subwavelength grating crossings for silicon wire waveguides," *Opt. Exp.*, vol. 18, no. 15, p. 16146, Jul. 2010.

[156] V. Donzella, A. Sherwali, J. Flueckiger, S. Talebi Fard, S. M. Grist, and L. Chrostowski, "Sub-wavelength grating components for integrated optics applications on SOI chips," *Opt. Exp.*, vol. 22, no. 17, p. 21037, Aug. 2014.

[157] R. Halir, A. Maese-Novo, A. Ortega-Moñux, I. Molina-Fernández, J. G. Wangüemert-Pérez, P. Cheben, D.-X. Xu, J. H. Schmid, and S. Janz, "Colorless directional coupler with dispersion engineered sub-wavelength structure," *Opt. Exp.*, vol. 20, no. 12, p. 13470, Jun. 2012.

[158] R. Halir, A. Ortega-Monux, J. H. Schmid, C. Alonso-Ramos, J. Lapointe, D.-X. Xu, J. G. Wanguemert-Perez, I. Molina-Fernandez, and S. Janz, "Recent advances in silicon waveguide devices using sub-wavelength gratings," *IEEE J. Sel. Topics Quantum Electron.*, vol. 20, no. 4, pp. 279–291, Jul. 2014.

[159] J. Wang, I. Glesk, and L. R. Chen, "Subwavelength grating filtering devices," *Opt. Exp.*, vol. 22, no. 13, p. 15335, Jun. 2014.

[160] Y. Wang, H. Sun, M. Khalil, W. Dong, I. Gasulla, J. Capmany, and L. R. Chen, "On-chip optical true time delay lines based on sub-wavelength grating waveguides," *Opt. Lett.*, vol. 46, no. 6, p. 1405, Mar. 2021.

[161] J. Wang, R. Ashrafi, R. Adams, I. Glesk, I. Gasulla, J. Capmany, and L. R. Chen, "Subwavelength grating enabled on-chip ultra-compact optical true time delay line," *Sci. Rep.*, vol. 6, no. 1, p. 30235, Sep. 2016.

[162] J. T. Mok and B. J. Eggleton, "Expect more delays," *Nature*, vol. 433, no. 7028, pp. 811–812, Feb. 2005.

[163] J. B. Khurgin, "Slow light in various media: A tutorial," *Adv. Opt. Photon.*, vol. 2, no. 3, p. 287, Sep. 2010.
[164] R. W. Boyd, *Nonlinear Optics*. San Diego, CA: Academic, 2003.
[165] Y. Okawachi, M. A. Foster, X. Chen, A. C. Turner-Foster, R. Salem, M. Lipson, C. Xu, and A. L. Gaeta, "Large tunable delays using parametric mixing and phase conjugation in Si nanowaveguides," *Opt. Exp.*, vol. 16, no. 14, p. 10349, Jul. 2008.
[166] C. Zhu, L. Lu, W. Shan, W. Xu, G. Zhou, L. Zhou, and J. Chen, "Silicon integrated microwave photonic beamformer," *Optica*, vol. 7, no. 9, p. 1162, Sep. 2020.
[167] L. Zhou, X. Wang, L. Lu, and J. Chen, "Integrated optical delay lines: A review and perspective," *Chin. Opt. Lett.*, vol. 16, no. 10, Oct. 2018, Art. no. 101301.
[168] H. Park, J. P. Mack, D. J. Blumenthal, and J. E. Bowers, "An integrated recirculating optical buffer," *Opt. Exp.*, vol. 16, no. 15, p. 11124, Jul. 2008.
[169] T. Tanemura, I. M. Soganci, T. Oyama, T. Ohyama, S. Mino, K. A. Williams, N. Calabretta, H. J. S. Dorren, and Y. Nakano, "Large-capacity compact optical buffer based on InP integrated phased-array switch and coiled fiber delay lines," *J. Lightw. Technol.*, vol. 29, no. 4, pp. 396–402, Feb. 1, 2011.
[170] M. Moralis-Pegios, G. Mourgias-Alexandris, N. Terzenidis, M. Cherchi, M. Harjanne, T. Aalto, A. Miliou, N. Pleros, and K. Vyrsokinos, "On-chip SOI delay line bank for optical buffers and time slot interchangers," *IEEE Photon. Technol. Lett.*, vol. 30, no. 1, pp. 31–34, Jan. 1, 2018.
[171] J. Capmany, J. Mora, I. Gasulla, J. Sancho, J. Lloret, and S. Sales, "Microwave photonic signal processing," *J. Lightw. Technol.*, vol. 31, no. 4, pp. 571–586, Feb. 15, 2013.
[172] J. Yao, "Photonics to the rescue: A fresh look at microwave photonic filters," *IEEE Microw. Mag.*, vol. 16, no. 8, pp. 46–60, Sep. 2015.
[173] L. R. Chen, "Silicon photonics for microwave photonics applications," *J. Lightw. Technol.*, vol. 35, no. 4, pp. 824–835, Feb. 15, 2017.

BANAFUL PAUL (Student Member, IEEE) received the B.Sc. degree in electrical and electronics engineering from the Chittagong University of Engineering and Technology, Chittagong, Bangladesh, in 2012, and the M.Sc. degree in electrical and computer engineering from The University of Texas at Dallas, Dallas, TX, USA, in 2018, with a focus on passively mode-locked semiconductor lasers. He is currently pursuing the Ph.D. degree in electrical and computer engineering with The Ohio State University, Columbus, OH, USA.

He is a Graduate Research Associate with the ElectroScience Laboratory, The Ohio State University. His research interests include silicon photonics, wideband beamforming for mmWave and sensing, and high frequency III–V mode-locked lasers.

KUBILAY SERTEL (Senior Member, IEEE) received the Ph.D. degree from the Department of Electrical Engineering and Computer Science, University of Michigan, Ann Arbor, MI, USA, in 2003.

He was an Assistant Professor with The Ohio State University, Columbus, OH, USA, from 2012 to 2017, where, he was a Research Scientist with the ElectroScience Laboratory and an Adjunct Professor with the Electrical and Computer Engineering Department, from 2003 to 2012. He is currently an Associate Professor with the Electrical and Computer Engineering Department, The Ohio State University. He has coauthored two books, such as *Integral Equation Methods for Electromagnetics* (SciTech Publishing, 2012) and *Frequency Domain Hybrid Finite Element Methods in Electromagnetics* (Morgan & Claypool, 2006), eight book chapters, and four patents. He has published over 90 journal articles and more than 300 conference papers. His current research interests include the analysis and design of THz and mmW sensors, imaging and radars, on-wafer noncontact metrology systems for device and IC testing, biomedical applications of THz imaging, and spectroscopy techniques for nondestructive evaluation. His research interests also include ultrawideband low-profile phased arrays for cognitive sensing and opportunistic wireless networks, reconfigurable antennas and arrays, applied electromagnetic theory, and computational electromagnetics, particularly, curvilinear fast multipole modeling of hybrid integral equation/finite element systems, efficient solutions of large-scale, and real-life problems on massively parallel supercomputing platforms.

He is a member of the IEEE Antennas and Propagation and Microwave Theory and Techniques Societies and an Elected Member of the URSI Commission B. He is also a fellow of the Applied Computational Electromagnetics Society. He serves as the Editor-in-Chief for Electronic Publications for the IEEE Antennas and Propagation Society.

NIRU K. NAHAR (Senior Member, IEEE) received the B.Sc. degree (Hons.) in physics from Dhaka University, Bangladesh, the M.S. degree in physics from the Indiana University of Pennsylvania, Indiana, PA, USA, and the M.S. and Ph.D. degrees in electrical and computer engineering from The Ohio State University (OSU), in 2002 and 2008, respectively.

She has been a Researcher with the ElectroScience Laboratory, since 2008. She is currently a Research Assistant Professor with the ElectroScience Laboratory, Electrical and Computer Engineering Department, OSU. She has worked as a Research Intern at the Surface Analysis Laboratory, Chemical and Metallurgical Division, Osram Sylvania Inc., Towanda, PA, USA. She has over three years of research experience in optometry and vision science. She has authored one book, one book chapter, three patents, 40 journal articles, and over 100 conference proceedings and abstracts. Her current research interests include the designs and characterization of THz and mmW sensors, THz spectroscopy systems for biomedical imaging, mmW ultra-wideband low-profile antennas and phased arrays for cognitive sensing, automobile RADAR, reconfigurable arrays, and novel RF-EO sensors. She has graduated six Ph.D. and four M.S. students. She has been an Elected Member of URSI Commission B, since 2016. She is a Senior Member of The Optical Society (OSA). She is a member of IEEE Antennas and Propagation Society and IEEE Lasers and Electro-Optics. In 2015, she was awarded the Lumley Research Award from the College of Engineering, OSU, for her outstanding research. She has served as a Secretary/Treasurer, the Vice Chairman, and the Chairman for IEEE Joint AP/MTT Chapter Columbus Section, from 2011 to 2014.